SPIN
Vol. 10, No. 3 (2020) 2050022 (12 pages)

DOI: 10.1142/S2010324720500228

World Scientific
www.worldscientific.com

First-Principles Study of the New Half-Metallic Ferromagnetic Quaternary-Heusler Alloys NaXNO (X = Ca, Sr, Ba)

K. Belkacem*, Y. Zaoui*, S. Amari*,†,‡, L. Beldi* and B. Bouhafs*
*Modeling and Simulation in Materials Science Laboratory
Physics Department
Djillali Liabès University of Sidi Bel-Abbès
Sidi Bel-Abbès 22000, Algeria

†Faculty of Nature and Life Science
Hassiba Benbouali University of Chlef Ouled Fares
Chlef 02000, Algeria
‡siham_amari@yahoo.fr

Received 23 March 2020
Accepted 28 June 2020
Published 19 August 2020

The first-principles approach based on density functional theory (DFT) and the full-potential linearized augmented plane-wave method were employed to investigate the structural, elastic, electronic and magnetic properties of NaXNO (X = Ca, Sr and Ba) quaternary half-Heusler alloys. The generalized gradient approximation (GGA) as parameterized by Perdew, Burke and Ernzerhof (PBE) and the modified Becke–Johnson exchange potential were used. As far as we know, we present our results which for the first time quantitatively account for the electronic structures and magnetic properties of NaXNO (X = Ca, Sr and Ba) quaternary half-Heusler alloys. From the total energy calculation using three possible atomic configurations (α, β and γ), it is found that the NaXNO (X = Ca, Sr and Ba) quaternary half-Heusler alloys are more stable in the ferromagnetic γ-phase. From our estimated elastic constants C_{ij}, it is found that all the considered Heusler alloys are mechanically stable in the γ-phase. We have also investigated the robustness of the half-metallicity with respect to the variation of lattice constants in these alloys. We have found that these alloys are half-metallic ferromagnets (HMFs) with a magnetic moment of 2 μ_B per formula unit at their equilibrium volumes. The spin-polarized electronic band structure and density of states of these quaternary half-Heusler alloys calculated by GGA (mBJ-GGA) show that the minority spin channels have metallic nature and the majority spin channels have a semiconductor character with half-metallic gaps of 0.49 eV (2.17 eV), 0.72 eV (2.28 eV) and 0.96 eV (2.22 eV) for NaCaNO, NaSrNO and NaBaNO quaternary half-Heusler alloys, respectively. Analysis of the density of states and the spin charge density of these quaternary alloys indicates that their magnetic moments mainly originate from the strong spin-polarization of 2p states of N atoms and O atoms.

Keywords: Density functional theory; Heusler alloys; half-metallic ferromagnets; magnetism.

‡Corresponding author.

1. Introduction

Recently, we have shown that many compounds exhibit half-metallic (HM) nature without the partially filled d atomic orbitals such as the alkaline earth carbides and nitride binary compounds.[1–3] The magnetism related to the p atomic orbitals has been also found in the half-Heusler XYZ,[4–10] the full-Heusler X_2YZ[11–15] and the equiatomic quaternary-Heusler $XX'YZ$[16,17] alloys.

The spintronic devices based on Heusler alloys require the development of new alloys that show ferromagnetism behavior using elements which are intrinsically nonmagnetic,[4–17] or the transition metal elements.[18–21] The Heusler alloys without transition metals mainly referred to as the d^0 half-metallic ferromagnets (HMFs) still constitute a field of active research.[22,23] They have attracted great interest due to their possible applications in spintronics.[24–28] This class of alloys is strongly ferromagnetic (FM) made by combining nonmagnetic elements[29–32] compared to that predicted by de Groot *et al.* in 1983.[29]

It is well known that the quaternary half-Heusler $XX'YZ$ alloys adopt the LiMgPdSn-type crystal structure[33–37] with $F\bar{4}3m$ (No. 216) space group and Wyckoff positions $X(0,0,0)$, $X'(1/2,1/2,1/2)$, $Y(1/4,1/4,1/4)$ and $Z(3/4,3/4,3/4)$. Although none of their constituent elements are magnetic, this new class of ordered alloys remains until now a subject of great theoretical and technological interest, due to their ferromagnetic behavior and the half-metallic character that they exhibit.

Based on the first-principles electronic structure calculations, many half-Heusler alloys which do not contain $3d$ transition metals were predicted theoretically to be HMFs. Recently, using the full-potential local-orbital (FPLO) method, Wei *et al.*[6] have reported the stability, electronic as well as magnetic properties of CNaCa and SiNaCa ternary-Heusler alloys. GeKCa and SnKCa half-Heusler alloys were found to be half-metallic ferromagnets by first-principles calculations.[38]

To the best of our knowledge, there are no experimental or theoretical studies on the NaXNO (X = Ca, Sr and Ba) quaternary half-Heusler alloys. Thus, we employ first-principles calculations based on density functional theory (DFT) with spin-polarization to explore the structural, electronic, elastic and magnetic properties of the NaXNO (X = Ca, Sr and Ba) quaternary half-Heusler alloys. We found that NaXNO (X = Ca, Sr, Ba) quaternary half-Heusler alloys are half-metals, with potential application prospect in spintronic devices. The paper is organized as follows: Section 2 details the computational method employed in this work. The possible crystal structures of the NaXNO (X = Ca, Sr and Ba) quaternary half-Heusler alloys and the results obtained are presented and discussed in Sec. 3, followed by some concluding remarks in Sec. 4.

2. Computational Details

In this study, we have performed first-principles total energy calculations within the DFT[39,40] using the full-potential linearized augmented plane-wave plus local orbitals (FP-LAPW) method as implemented in the WIEN2K package.[41] The exchange–correlation energy was described with the Perdew–Burke–Ernzerhof generalized gradient approximation (GGA-PBE)[42] and the modified Becke–Johnson (mBJ) approach.[43] The orbitals, charge density and potential were expanded using spherical harmonics in the muffin-tin (MT) spheres. Plane waves were used in the description of the interstitial region.

The electronic configurations of each element in the NaXNO (X = Ca, Sr and Ba) quaternary half-Heusler alloys used in this study are Na: [Ne]$3s^1$, Ca: [Ar]$4s^2$, Sr: [Kr]$5s^2$, Ba: [Xe]$6s^2$, N: [He]$2s^2 2p^3$ and O: [He]$2s^2 2p^4$. The MT radii of 2.50 bohr for Na and X (Ca, Sr and Ba) and 2.00 bohr for N and O were adopted. A set of meshes of $11 \times 11 \times 11$ Monkhorst−Pack[44] special k-points for the cubic α-, β- and γ-phases were used for the Brillouin zone (BZ) integration in order to obtain converged energies. The value of 9.0 for $R_{\mathrm{MT}} \times K_{\mathrm{MAX}}$ was used for all the considered phases. The self-consistent calculations are converged up to 0.001 mRy. The total density of states (DOS) was obtained using the modified tetrahedron method[45] with a dense mesh of $17 \times 17 \times 17$ k-points for the stable γ-phase.

The mechanical properties which include the elastic constants (C_{ij}) are of fundamental importance when considering phase stability at a given pressure. The mechanical property calculations of the NaXNO (X = Ca, Sr and Ba) quaternary half-Heusler alloys in the γ-phase were carried out using the supercell approach in the framework of Hellmann–Feynman theorem[46] as implemented in the WIEN2K code[41] which consists in evaluating the

forces due to the finite displacement of an atom from its equilibrium position.

3. Results and Discussion

3.1. *Structural and magnetic properties*

The nonspin-polarized (NSP) and spin-polarized (SP) total energies as a function of volume of the considered NaXNO (X = Ca, Sr and Ba) quaternary half-Heusler alloys are calculated in the cubic α-, β- and γ-phases (see Fig. 1). The total energies as a function of volume for the FM and nonmagnetic (NM) configurations in these three phases are presented in Fig. 2. From Fig. 2, it is clear that the FM phases of all considered quaternary half-Heusler alloys are most favorable than the NM phases, and that the γ-phase is most stable than the α- and β-phases. The structural properties were determined by fitting the total energy versus volume using the Murnaghan[47] equation of states. Our calculated equilibrium lattice parameters, bulk moduli and their first derivatives for the NM and FM configurations are reported in Table 1. The calculated lattice parameters and bulk moduli of the NaXNO (X = Ca, Sr and Ba) quaternary half-Heusler alloys in the considered α-, β- and γ-phases increase and decrease, respectively, with varying X in the following order: Ca → Sr → Ba.

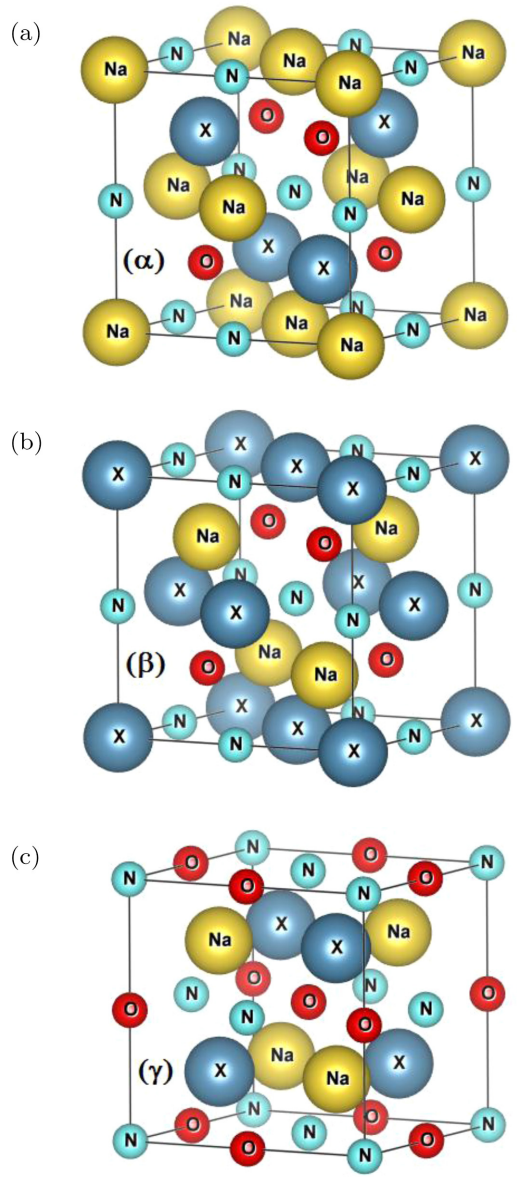

Fig. 1. Schematics of crystal structures of NaXNO (X = Ca, Sr and Ba) quaternary half-Heusler alloys in the (a) α-phase, (b) β-phase and (c) γ-phase.

We have also evaluated the formation energy of the NaXNO (X = Ca, Sr and Ba) quaternary half-Heusler alloys in the α-, β- and γ-phases using the following equation[1,3]:

$$E_f^{\mathrm{Na}X\mathrm{NO}} = E_{\mathrm{tot}}^{\mathrm{Na}X\mathrm{NO}} - E_{\mathrm{Na}}^{\mathrm{bulk}} + E_X^{\mathrm{bulk}} + E_{\mathrm{N}}^{\mathrm{bulk}} + E_{\mathrm{O}}^{\mathrm{bulk}}, \tag{1}$$

where $E_{\mathrm{tot}}^{\mathrm{Na}X\mathrm{NO}}$ is the equilibrium total energy of the NaXNO (X = Ca, Sr and Ba) quaternary half-Heusler alloys, whereas $E_{\mathrm{Na}}^{\mathrm{bulk}}$, E_X^{bulk}, $E_{\mathrm{N}}^{\mathrm{bulk}}$ and $E_{\mathrm{O}}^{\mathrm{bulk}}$ are the total energies of Na, X (where X can be Ca, Sr or Ba), N and O atoms, respectively, in their bulk phases. Note that we adopt the fcc phase (Fm-3m) for Ca and Sr, the cc phase (Im-3m) for Ba, the γ-phase ($P4_2/mnm$) for the ground state of solid nitrogen[48]and the cubic phase (Pm-3n) for O_2 in the calculations of their total energies. Negative value of the formation energy gives an indication on the stability of the quaternary half-Heusler alloys. In Table 1, we have reported the calculated values of the formation energy. We found that the calculated formation energies E_f for all considered phases (α, β and γ) of NaCaNO, NaSrNO and NaBaNO alloys are −1.11 eV/atom, −1.06 eV/atom and −1.05 eV/atom, respectively, which indicate that these alloys are thermodynamically stable due to their lower negative formation energies and they will not decompose once they have been formed.

The cohesive energies of the NaXNO (X = Ca, Sr and Ba) quaternary half-Heusler alloys in the α-, β- and γ-phases have been also computed using the

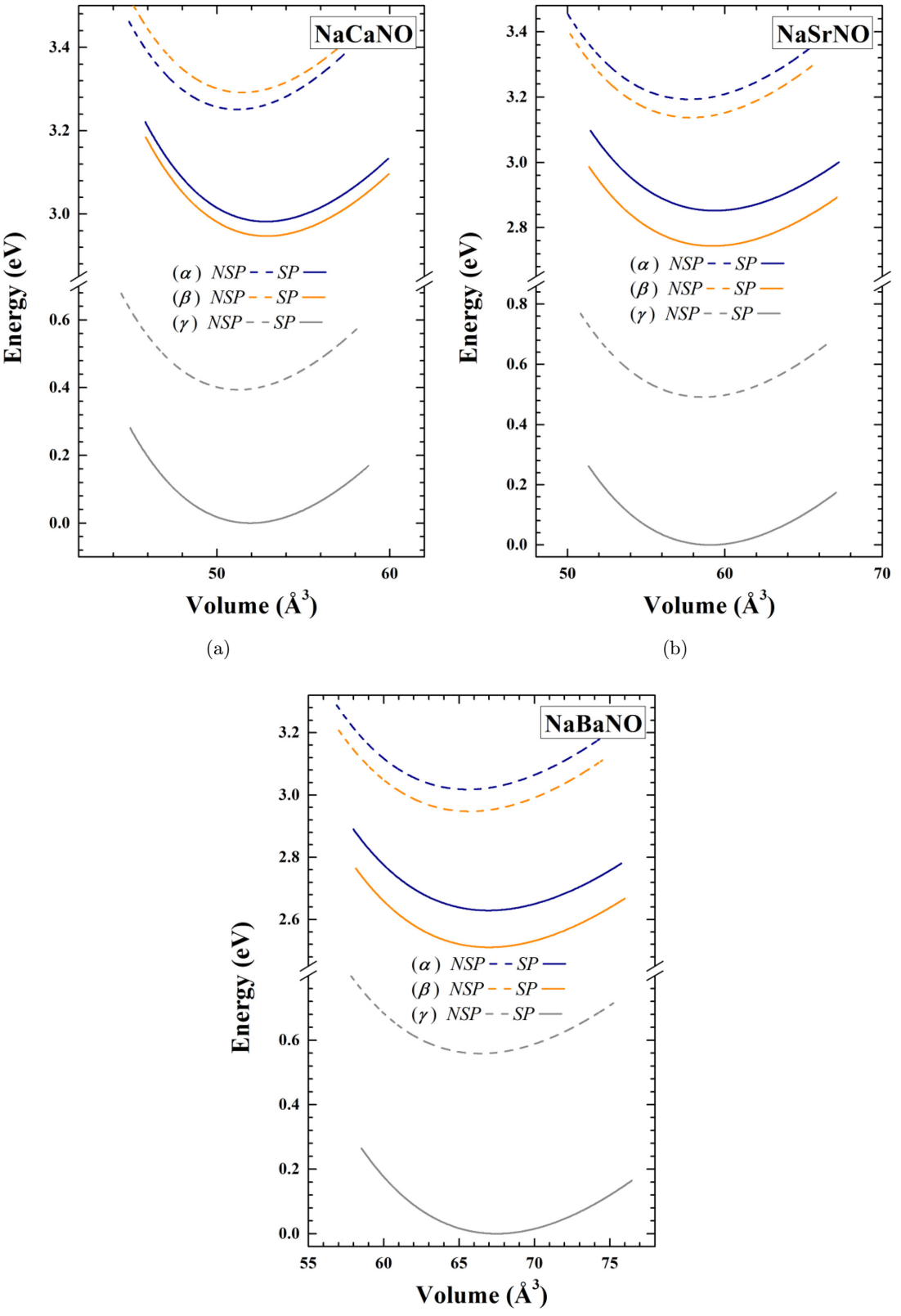

Fig. 2. Total energy as a function of volume per formula unit for the nonspin-polarized and spin-polarized spin configurations of (a) NaCaNO, (b) NaSrNO and (c) NaBaNO quaternary half-Heusler alloys in the α-, β- and γ-phases using GGA-PBE.

Table 1. The spin-polarized and nonspin-polarized calculation results using GGA-PBE of the lattice parameter (a, in Å), bulk modulus (B, in GPa), its pressure derivative (B'), total magnetic moment per formula unit μ_{tot} (in μ_{B}/cell), local magnetic moments μ_{N} and μ_{O} (in μ_{B}/atom) of N and O atoms, respectively, spin-polarization energy $\Delta E^{\text{FM-NM}}$ (in meV/f.u.), cohesive energy (E_{coh}, in eV/atom) and formation energy (E_f, in eV/atom) of NaCaNO, NaSrNO and NaBaNO quaternary half-Heusler alloys given in different phases α, β and γ.

			a	B	B'	μ_{tot}	μ_{N}	μ_{O}	$\Delta E^{\text{FM-NM}}$	E_{coh}	E_f
NaCaNO	α	NSP	5.89	69	4.52						
		SP	5.96	64	4.50	2	1.15	0.68	−269	5.40	−1.11
	β	NSP	5.90	68	4.38						
		SP	5.96	63	4.45	2	1.19	0.61	−345	5.40	−1.11
	γ	NSP	5.90	78	4.35						
		SP	5.92	74	4.32	2	1.23	0.55	−394	5.40	−1.11
NaSrNO	α	NSP	6.13	62	4.59						
		SP	6.19	57	4.62	2	1.20	0.63	−341	5.27	−1.06
	β	NSP	6.14	62	4.61						
		SP	6.19	57	4.62	2	1.20	0.60	−394	5.27	−1.06
	γ	NSP	6.17	66	4.39						
		SP	6.18	64	4.42	2	1.25	0.52	−491	5.27	−1.06
NaBaNO	α	NSP	6.40	56	4.94						
		SP	6.45	52	4.72	2	1.24	0.58	−389	5.26	−1.05
	β	NSP	6.40	56	4.58						
		SP	6.45	53	4.86	2	1.24	0.56	−437	5.26	−1.05
	γ	NSP	6.43	53	4.64						
		SP	6.46	55	4.34	2	1.28	0.47	−559	5.26	−1.05

following relation[1,3]:

$$E_c^{\text{Na}X\text{NO}} = -E_{\text{tot}}^{\text{Na}X\text{NO}} + E_{\text{Na}}^{\text{atom}} + E_X^{\text{atom}} + E_{\text{N}}^{\text{atom}} + E_{\text{O}}^{\text{atom}}, \quad (2)$$

where $E_{\text{tot}}^{\text{Na}X\text{NO}}$ is the equilibrium total energy of the NaXNO (X = Ca, Sr and Ba) quaternary half-Heusler alloys, whereas $E_{\text{Na}}^{\text{atom}}$, E_X^{atom}, $E_{\text{N}}^{\text{atom}}$ and $E_{\text{O}}^{\text{atom}}$ are the total energies of isolated atoms. The values of E_c represented in Table 1 confirm the structural stability of the quaternary half-Heusler alloys in the α-, β- and γ-phases. The calculated cohesive energies for all the considered phases (α, β and γ) of NaCaNO, NaSrNO and NaBaNO alloys are 5.40 eV/atom, 5.27 eV/atom and 5.26 eV/atom, respectively, which are of lower magnitude. Moreover, according to our computed values, it is clear that the γ-phase needs more energy to be broken into free atoms than the α- and β-phases.

The calculated total magnetic moment μ_{tot} and local magnetic moments μ_{N} and μ_{O} of N and O atoms, respectively, of the NaXNO (X = Ca, Sr and Ba) quaternary half-Heusler alloys calculated in different phases α, β and γ are listed in Table 1. The results show that the main contribution to the total magnetic moment comes from the N atoms with small contribution from the O atoms. It is clear that all considered quaternary half-Heusler alloys exhibit integer total magnetic moments of 2 μ_B, indicating that these quaternary half-Heusler alloys can be HMFs. Figure 3 shows that during the variation of the total magnetic moment μ_{tot} and the local magnetic moments μ_{N} and μ_{O} with the lattice constants of NaCaNO, NaSrNO and NaBaNO quaternary half-Heusler alloys in the stable γ-phase, they retain their integer values with the compression and expansion of the lattice constant around the equilibrium value.

3.2. *Elastic properties*

We have calculated the elastic constants C_{ij}, as well as the relative mechanical parameters, such as the bulk modulus, the shear modulus G, the Young's modulus E, the Poisson's ratio ν and Pugh's ratio (G/B) using the Hill approach.[49] From the inspection of Table 2, we can notice that our calculated values of the elastic constants satisfy the Born–Huang[50] mechanical stability conditions, indicating that all the considered alloys are mechanically stable in the given γ-phase. Furthermore, we notice from our computed mechanical parameters reported in

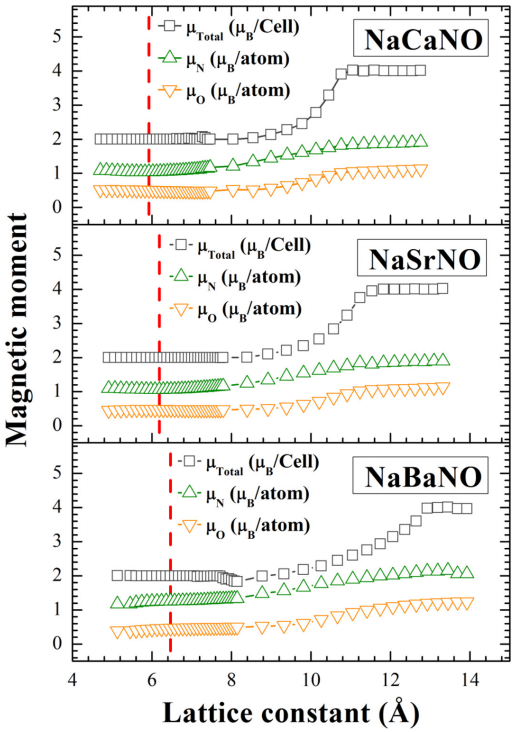

Fig. 3. The variations of the total magnetic moment $\mu_{\rm tot}$ and the local magnetic moments $\mu_{\rm N}$ and $\mu_{\rm O}$ of N and O atoms of NaCaNO, NaSrNO and NaBaNO quaternary half-Heusler alloys as a function of the lattice constant in the stable γ-phase. The vertical dashed lines indicate the equilibrium lattice constants.

Table 2. The calculated elastic constants C_{ij}, elastic moduli B, G and E (in GPa) and the Poisson's ratio ν for NaCaNO, NaSrNO and NaBaNO quaternary half-Heusler alloys given in the γ-phase using GGA-PBE at zero pressure. The elastic moduli and Poisson's ratios are given in the Hill approximation.

	C_{11}	C_{12}	C_{44}	B_H	G_H	E_H	ν_H	θ_D	G_H/B_H
NaCaNO	137	45	16	76	25	67	0.35	410	0.33
NaSrNO	111	43	17	65	22	60	0.35	324	0.34
NaBaNO	85	41	6	56	11	30	0.41	199	0.19

Table 2 that the lowest value of Young's modulus E among the NaXNO (X = Ca, Sr and Ba) alloys is 30 GPa for NaBaNO which means that this alloy is stiffer than NaCaNO and NaBaNO alloys whose Young's modulus values are 60 GPa and 67 GPa, respectively.

According to the criteria of Pugh[51] and Frantsevich *et al.*,[52] a compound is ductile if its Pugh's ratio value is lower than 0.57 and Poisson's ratio is higher than 0.26, respectively. It is clear that all the calculated values of Pugh's ratio are less than 0.57, as well as the values of Poisson's ratio are higher than 0.26, indicating that all the considered alloys are ductile in nature (see Table 2). Our calculated values of Poisson's ratio indicate the presence of weak ionic bonding character in NaCaNO and NaSrNO alloys since their Poisson's ratio values meet the lower limit of $v = 0.33$. To our knowledge, there are no experimental or theoretical data to compare our results.

3.3. *Band structures and density of states*

The spin-polarized band structures for both majority and minority spin channels of NaCaNO, NaSrNO and NaBaNO quaternary half-Heusler alloys were calculated at their respective equilibrium lattice constants in the stable γ-phase using GGA-PBE and mBJ-GGA-PBE, as shown in Fig. 4. The band structures calculated using GGA-PBE and the mBJ-GGA-PBE have similar topologies, with the conduction and valence bands being shifted up and down with respect to the Fermi level, respectively, which induces a widening of the gap. Figure 4 indicates that the NaXNO (X = Ca, Sr and Ba) quaternary half-Heusler alloys in both GGA-PBE and mBJ-GGA-PBE exhibit a HM behavior with 100% spin-polarization around the Fermi level. We found that the minority spin channel exhibits a metallic behavior, whereas the majority spin channel presents wide indirect bandgaps of 5.19 eV (7.50 eV), 4.71 eV (7.79 eV) and 4.63 eV (6.93 eV) using GGA-PBE (mBJ-GGA-PBE) for the NaCaCCl, NaSrCCl and NaBaCCl alloys, respectively. The values of the energy bandgap reported in Table 3 are larger using mBJ-GGA-PBE compared to GGA-PBE. The HM gap values of the considered quaternary half-Heusler alloys using both GGA-PBE and mBJ-GGA-PBE are reported in Table 3. The calculated values of HM gaps at the equilibrium lattice parameters are 0.49 eV (2.17 eV), 0.72 eV (2.28 eV) and 0.96 eV (2.22 eV) using GGA-PBE (mBJ-GGA-PBE) for the NaCaNO, NaSrNO and NaBaNO quaternary half-Heusler alloys, respectively.

The calculated total magnetic moment ($\mu_{\rm tot}$) satisfies the rule of the Slater–Pauling behavior in the quaternary half-Heusler alloys.[53] In this rule, $\mu_{\rm tot}$ is related to the total valence electrons ($Z_{\rm tot}$) of the Heusler alloys. The total magnetic moment $\mu_{\rm tot}$

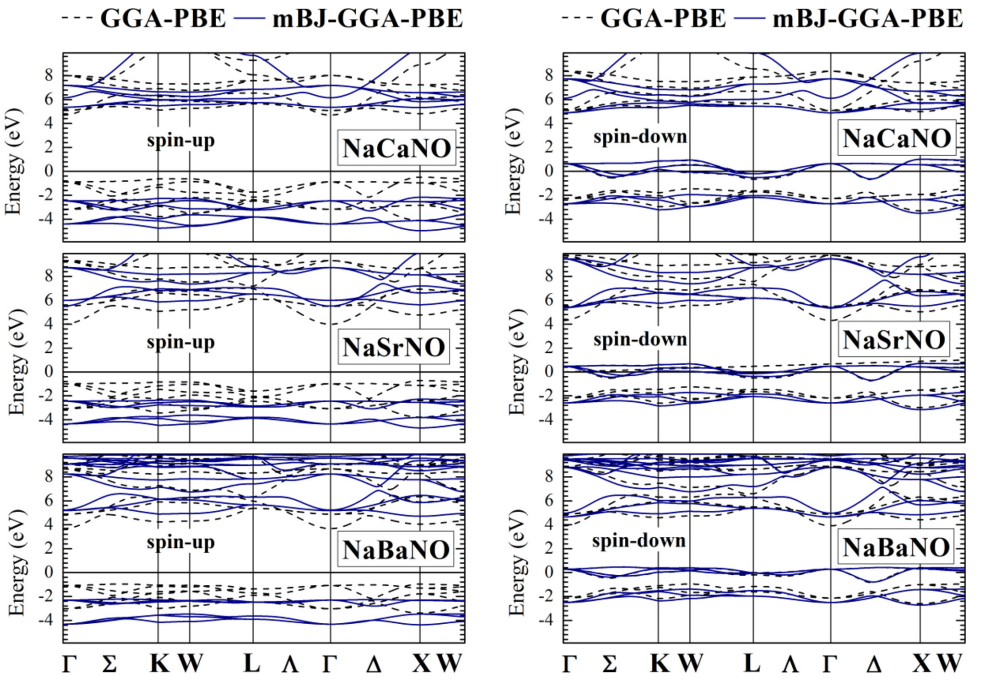

Fig. 4. Comparison of GGA-PBE (dashed line) and mBJ-GGA-PBE (solid line) spin-polarized band structures for both majority (left-hand side) and minority (right-hand side) spin channels of NaCaNO, NaSrNO and NaBaNO quaternary half-Heusler alloys calculated in the stable γ-phase. The horizontal dashed line indicates the Fermi level.

Table 3. The total magnetic moment per formula unit $\mu_{\rm tot}$ (in $\mu_{\rm B}$/cell), local magnetic moments $\mu_{\rm N}$ and $\mu_{\rm O}$ (in $\mu_{\rm B}$/atom) of N and O atoms, respectively, energy bandgap (E_g, in eV) and the half-metallic gap ($E_g^{\rm HM}$, in eV) of the NaCaNO, NaSrNO and NaBaNO quaternary half-Heusler alloys calculated using GGA-PBE and mBJ-GGA-PBE in the stable γ-phase.

		$\mu_{\rm tot}$	$\mu_{\rm N}$	$\mu_{\rm O}$	E_g	VBM → CBM	$E_g^{\rm HM}$
NaCaNO	GGA-PBE	2	1.23	0.55	5.19	$W \to X$	0.49
	mBJ-GGA-PBE	2	1.55	0.58	7.50	$W \to X$	2.17
NaSrNO	GGA-PBE	2	1.25	0.52	4.71	$W \to \Gamma$	0.72
	mBJ-GGA-PBE	2	1.58	0.53	7.79	$W \to \Gamma$	2.28
NaBaNO	GGA-PBE	2	1.28	0.47	4.63	$\Delta \to \Gamma$	0.96
	mBJ-GGA-PBE	2	1.61	0.48	6.93	$\Delta \to \Gamma$	2.22

is calculated as[11]

$$\mu_{\rm tot} = (N\uparrow - N\downarrow)\mu_{\rm B} = (2N\uparrow - Z_{\rm tot})\mu_{\rm B}$$
$$= (16 - Z_{\rm tot})\mu_{\rm B}. \quad (3)$$

NaXNO (X = Ca, Sr and Ba) quaternary half-Heusler alloys have 14 valence electrons in the unit cell [one from Na, two from X (X = Ca, Sr or Ba) atom, five from N atom and six from O atom]. According to Eq. (3), $\mu_{\rm tot}$ is equal to 2 $\mu_{\rm B}$ for all the considered quaternary half-Heusler alloys, which are in good agreement with the results of Table 1; as expected, the considered quaternary half-Heusler alloys exhibit an integer magnetic moment.

On the other hand, the Na and X atoms lose their electrons of the s-orbitals, while the N and O atoms obtain them. For the N atom, two electrons occupy the 2s-orbital and three electrons occupy the 2p-orbital; while for the O atom, two electrons occupy the 2s-orbital and the fourth electron occupies the 2p-orbital. According to Hund's rules, the majority spin N-2p and O-2p states are fully filled by three electrons, while the minority spin 2p-states are partially filled by two electrons with one hole. The total magnetic moment of the considered quaternary half-Heusler alloys is thus 2.0 $\mu_{\rm B}$/f.u.

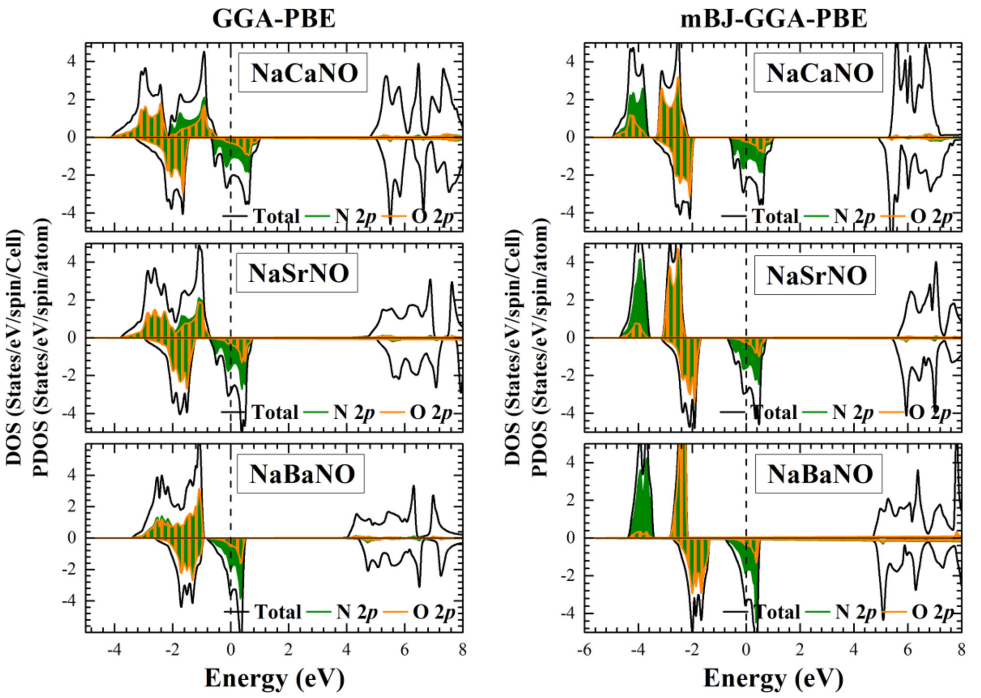

Fig. 5. The calculated spin-polarized total DOSs and PDOSs of NaCaNO, NaSrNO and NaBaNO quaternary half-Heusler alloys calculated in the stable γ-phase using GGA-PBE (left-hand side) and mBJ-GGA-PBE (right-hand side). The vertical dashed lines indicate the Fermi level. The positive (negative) DOS values correspond to the spin-up (spin-down) states.

The calculated spin-polarized total DOS and partial DOS (PDOS) values of NaCaNO, NaSrNO and NaBaNO quaternary half-Heusler alloys calculated in the stable γ-phase using GGA-PBE and mBJ-GGA-PBE are shown in Fig. 5. Comparing the total DOS and PDOS spectra with the calculated band structures of the considered quaternary half-Heusler alloys, we can see that for the majority spin direction, the valence states' spectra are fully filled and exhibit a semiconducting nature, whereas in the minority spin direction, these states are partially filled and cross the Fermi level exhibiting a metallic nature. We can see from Fig. 5 that in the region around the Fermi level, the DOS pattern shows obvious spin splitting, which reconfirms the half-metallic nature of these quaternary half-Heusler alloys. The PDOS spectra in the region around the Fermi level are mainly due to the N-2p and O-2p state contributions, while the contributions of Na and X(X = Ca, Sr and Ba) atoms are small. This is consistent with the calculated band structures. For the N-2p and O-2p states, the majority spin states are fully occupied, while the minority states are partially occupied. Thus, the magnetism of NaXNO (X = Ca, Sr and Ba) Heusler alloys is largely provoked by the N-2p and O-2p electrons.

3.4. *Charge density*

We have also presented in Fig. 6 the effect of spin-polarization on the total valence charge densities of these three alloys in the γ-phase using GGA-PBE. The 2D contour plots show a higher concentration of spin charge densities for the majority and minority spin channels of the quaternary half-Heusler alloys along the X–N and X–O (X = Ca, Sr or Ba) bonds, and around the nitrogen and oxygen atoms compared to the X atoms. The 2D contour plots show spatially varying charge densities, but identical for both the majority ($\rho_\uparrow$) and minority ($\rho_\downarrow$) spin channels. The contour plots around the N and O atoms show spatially varying spin density which is a little bit different for the two spin channels. Inspection of the 2D contour plots of the valence charge densities of the quaternary half-Heusler alloys showed that there exist significant charge transfers from the X to N and O atoms. The differences in the electronegativity values between N and X atoms ($\chi_N - \chi_X \cong 2.0$) and between O and X atoms ($\chi_O - \chi_X \cong 2.5$) using the Pauling electronegativity scale[54] provide a greater ability to N and O atoms to attract the electrons, and consequently the bond charge maximum moves toward them, indicating that the large difference in

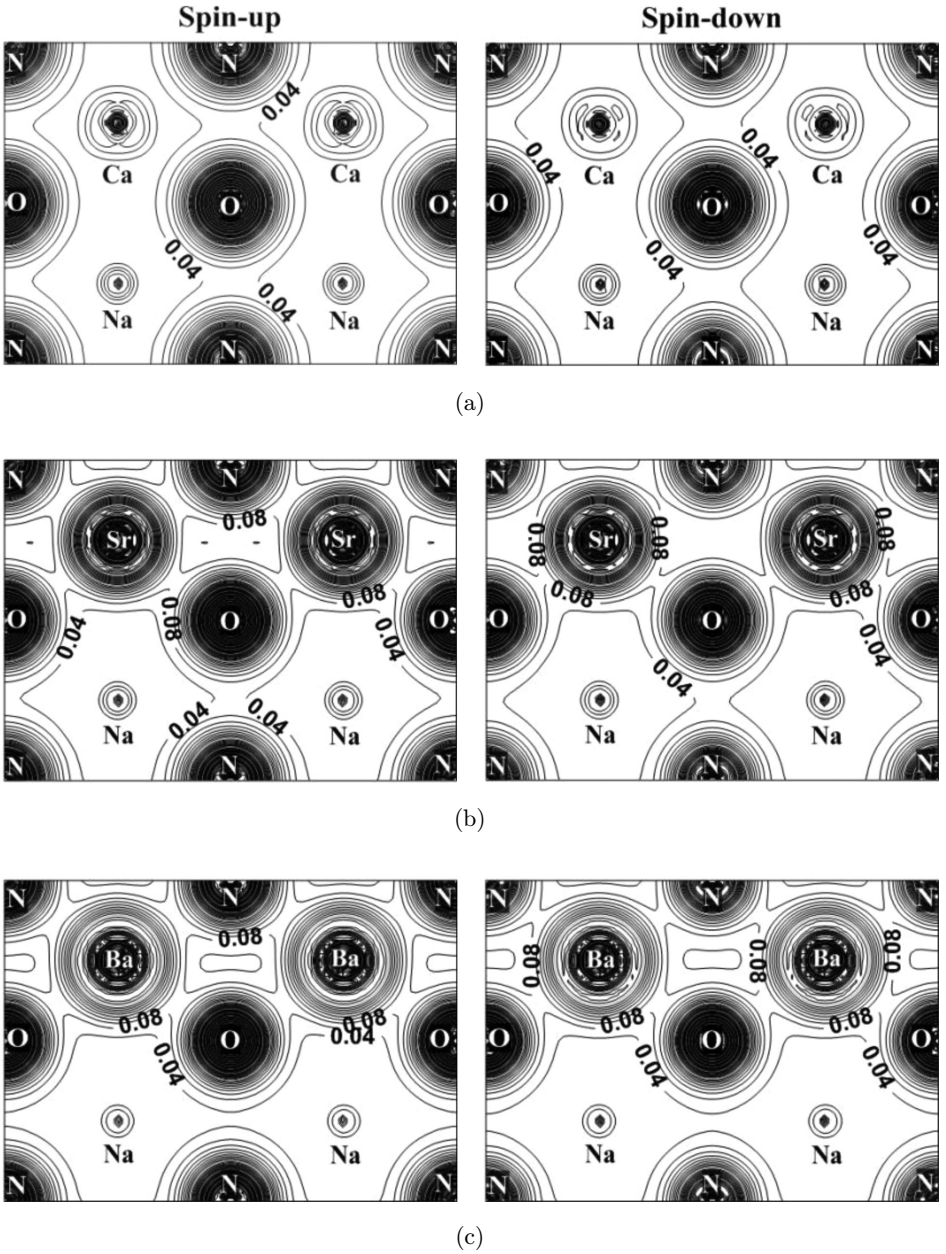

Fig. 6. Contour plots of the total valence charge densities of NaCaNO, NaSrNO and NaBaNO quaternary half-Heusler alloys calculated for the majority (left panel) and minority (right panel) spin configurations at their equilibrium lattice constants in the (110) plane of the stable γ-phase.

electronegativities is responsible for this charge transfer resulting in a ionic bond nature of these quaternary half-Heusler alloys.

From the electron density difference $(\rho_{\uparrow} - \rho_{\downarrow})$ [difference between majority $(\rho_{\uparrow})$ and minority $(\rho_{\downarrow})$ spin electrons' charge densities] contour plots, one can visualize the spin charge transfer of the quaternary half-Heusler alloys. From Fig. 7, we can see that the N and O sites are larger than the X sites for all cases. The contour plots are similar for the considered quaternary half-Heusler alloys with slight deviation in the spin charge difference near the N and O sites. The spin charge density calculations show that the majority $(\rho_{\uparrow})$ spin electrons' charge density differs slightly from the minority $(\rho_{\downarrow})$ spin electrons' charge density due to the spin distributions, therefore, the spin charge transfer is not similar in both the majority and minority spin channels. The overall shape of the contour plots, representing the spin charge distribution, suggests

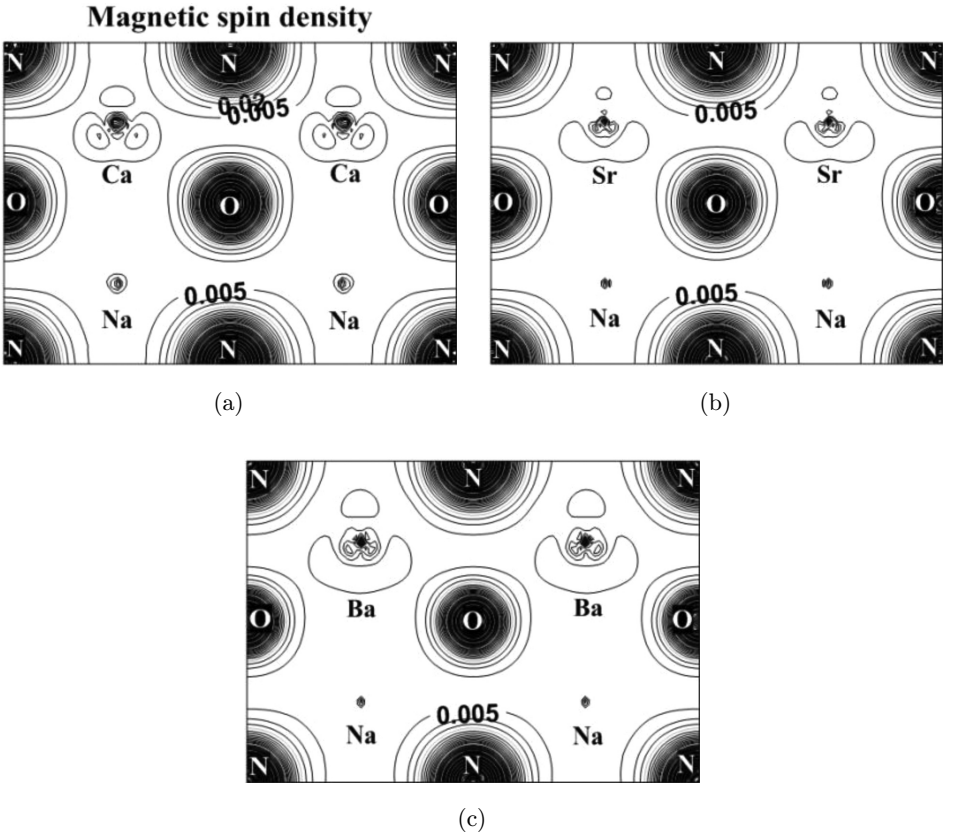

Fig. 7. Contour plots of the calculated total spin charge densities ($\rho_{\uparrow} - \rho_{\downarrow}$) of NaCaNO, NaSrNO and NaBaNO quaternary half-Heusler alloys calculated at their equilibrium lattice constants in the (110) plane of the stable γ-phase.

that magnetism originates from N and O atoms of the NaXNO (X = Ca, Sr and Ba) quaternary half-Heusler alloys.

4. Conclusions

In summary, a new class of d^0 magnetic quaternary half-Heusler alloys without transition metal elements was proposed in this paper. Using first-principles calculations, we investigated the structural, mechanical and electronic properties of the NaCaNO, NaSrNO and NaBaNO quaternary half-Heusler alloys in the α-, β- and γ-phases using the full-potential linearized augmented plane-wave plus local orbitals method within the GGA-PBE and mBJ-GGA-PBE approaches. We found that the ferromagnetic ground states are the most stable configurations for the NaCaNO, NaSrNO and NaBaNO quaternary half-Heusler alloys in the γ-phase. We have demonstrated through the minimization of the total energy of the three possible (α, β and γ) phases, as well as the calculation of the formation and cohesive energies, that the ferromagnetic γ-phase is the most favorable one. The calculated elastic constants meet the Born–Huang stability criteria and confirm that the considered alloys are mechanically stable. In addition, we found that the materials are ductile according to Pugh's criteria.

We found that these quaternary half-Heusler alloys present a half-metallic behavior in the γ-phase. The use of mBJ-GGA-PBE compared to GGA-PBE approximation results in a drastic change of the electronic structure of these alloys. The mBJ-GGA-PBE approximation corrects the half-metallic gap and the energy bandgap of the majority spin states. For the majority spin channel, these quaternary half-Heusler alloys show an indirect large bandgap and half-metallic gap. From the calculated DOS and spin charge densities, we have concluded that the magnetism in all considered quaternary half-Heusler alloys is attributed mainly to the partially filled $2p$-orbitals of the N and O atoms. We found that NaCaNO, NaSrNO and NaBaNO quaternary half-Heusler alloys have a ferromagnetic ground state configuration in the γ-phase, producing a total magnetic moment of $2\,\mu_{\mathrm{B}}$.

Acknowledgments

This work was supported by the Directorate General for Scientific Research and Technological Development (DGRSDT) of Algeria. B. Bouhafs acknowledges the Algerian Academy of Sciences and Technology (AAST) and the Abdus-Salam International Center for Theoretical Physics (ICTP, Trieste, Italy).

References

1. L. Beldi, H. Bendaoud, K. Obodo, B. Abbar and B. Bouhafs, *J. Supercond. Nov. Magn.* **32**, 2031 (2019).
2. L. Beldi, H. Bendaoud, K. Obodo, B. Abbar and B. Bouhafs, *Mater. Chem. Phys.* **237**, 121875 (2019).
3. L. Beldi, H. Bendaoud, K. Obodo, B. Bouhafs, S. Méçabih and B. Abbar, *Comput. Condens. Matter* **17**, e00336 (2018).
4. A. Lakdja, H. Rozale, A. Chahed and O. Benhelal, *J. Alloys Compd.* **564**, 8 (2013).
5. R. Umamaheswari, D. Vijayalakshmi and G. Kalpana, *Physica B* **448**, 256 (2014).
6. X.-P. Wei, Y.-D. Chu, X.-W. Sun, J.-B. Deng and Y.-Z. Xing, *Superlattices Microstruct.* **74**, 70 (2014).
7. R. Benabboun, D. Mesri, A. Tadjer, A. Lakdja and O. Benhelal, *J. Supercond. Nov. Magn.* **28**, 2881 (2015).
8. T. Malsawmtluanga, B. Vanlalruata and R. Thapa, *J. Phys., Conf. Ser.* **765**, 012018 (2016).
9. H. Rozale, M. Khetir, A. Amar, A. Lakdja, A. Sayede and O. Benhelal, *Superlattices Microstruct.* **74**, 146 (2014).
10. A. Lakdja, H. Rozale, A. Sayede and A. Chahed, *J. Magn. Magn. Mater.* **354**, 235 (2014).
11. S. Benatmane and B. Bouhafs, *Comput. Condens. Matter* **19**, e00371 (2019).
12. H. Rozale, A. Amar, A. Lakdja, A. Moukadem and A. Chahed, *J. Magn. Magn. Mater.* **336**, 83 (2013).
13. Y.-C. Gao, X.-T. Wang and H. Rozale, *Chin. Phys. B* **24**, 067102 (2015).
14. L. Zhang, X. Wang, H. Rozale, J.-W. Lu and L.-Y. Wang, *J. Supercond. Nov. Magn.* **28**, 3701 (2015).
15. L. Sun, *J. Supercond. Nov. Magn.*, 1 (2018).
16. J. Du, S. Dong, X. Wang, H. Zhao, L. Wang and L. Feng, *AIP Adv.* **6**, 105308 (2016).
17. J. Du, S. Dong, Y.-L. Lu, H. Zhao, L. Feng and L. Wang, *J. Magn. Magn. Mater.* **428**, 250 (2017).
18. S. Amari and B. Bouhafs, *J. Supercond. Nov. Magn.* **29**, 2311 (2016).
19. S. Amari, R. Mebsout, S. Méçabih, B. Abbar and B. Bouhafs, *Intermetallics* **44**, 26 (2014).
20. L. Seddik, S. Amari, K. Obodo, L. Beldi, H. Faraoun and B. Bouhafs, *SPIN* **7**, 1750010 (2017).
21. S. Amari, R. Mebsout, S. Méçabih, B. Abbar and B. Bouhafs, *Intermetallics* **37**, 27 (2013).
22. T. Graf, C. Felser and S. S. Parkin, *Prog. Solid State Chem.* **39**, 1 (2011).
23. T. Graf, F. Casper, J. Winterlik, B. Balke, G. H. Fecher and C. Felser, *Z. Anorg. Allg. Chem.* **635**, 976 (2009).
24. I. Žutić, J. Fabian and S. D. Sarma, *Rev. Mod. Phys.* **76**, 323 (2004).
25. A. Hirohata and K. Takanashi, *J. Phys. D, Appl. Phys.* **47**, 193001 (2014).
26. I. Galanakis, Theory of Heusler and full-Heusler compounds, in *Heusler Alloys*, eds. C. Felser and A. Hirohata, Springer Series in Materials Science, Vol. 222 (Springer International Publishing, 2016), pp. 3–36.
27. K. Westerholt, A. Bergmann, J. Grabis, A. Nefedov and H. Zabel, Magnetism and structure of magnetic multilayers based on the fully spin polarized Heusler alloys Co_2MnGe and Co_2MnSn, in *Half-Metallic Alloys*, eds. I. Galanakis and P. Dederichs, Lecture Notes in Physics, Vol. 676 (Springer, Berlin, 2005), pp. 67–112.
28. A. Hirohata, J. Sagar, L. Lari, L. R. Fleet and V. K. Lazarov, *Appl. Phys. A* **111**, 423 (2013).
29. R. A. de Groot, F. M. Mueller, P. G. van Engen and K. H. J. Buschow, *Phys. Rev. Lett.* **50**, 2024 (1983).
30. F. Heusler and E. Take, *Trans. Faraday Soc.* **8**, 169 (1912).
31. P. J. Webster and K. R. A. Ziebeck, Co_2YZ with Y = 3d element: Landolt-Börnstein — Group III condensed matter, in *Alloys and Compounds of d-Elements with Main Group Elements: Part 2*, ed. H. P. J. Wijn, Magnetic Properties of Metals, Vol. 19C (Springer-Verlag, Berlin, 1988), pp. a–b.
32. K. Ziebeck and K.-U. Neumann, in *Magnetic Properties of Metals: Alloys and Compounds of d-Elements with Main Group Elements — Part 2*, ed. H. J. S. Wijn, Landolt-Börnstein, New Series, Group III Condensed Matter, Vol. 32C (Springer, Berlin, 2001), pp. c–d.
33. S. Dong and H. Zhao, *Appl. Phys. Lett.* **100**, 142404 (2012).
34. G. Gao, K. Yao, Z. Liu, J. Zhang, Y. Min and S. Fan, *Phys. Lett. A* **372**, 1512 (2008).
35. R. A. de Groot, F. M. Mueller, P. G. van Engen and K. H. J. Buschow, *J. Appl. Phys.* **55**, 2151 (1984).
36. H. Nowotny and K. Bachmayer, *Monat.hefte Chem. — Chem. Mon.* **81**, 488 (1950).
37. F. Heusler, *Angew. Chem.* **17**, 260 (1904).
38. J. Chen, G. Gao, K. Yao and M. Song, *J. Alloys Compd.* **509**, 10172 (2011).
39. P. Hohenberg and W. Kohn, *Phys. Rev.* **136**, B864 (1964).

40. W. Kohn and L. J. Sham, *Phys. Rev.* **140**, A1133 (1965).
41. P. Blaha, K. Schwarz, G. K. H. Madsen, D. Kvasnicka, J. Luitz, R. Laskowski, F. Tran and L. D. Marks, *WIEN2k: An Augmented Plane Wave + Local Orbitals Program for Calculating Crystal Properties* (Technische Universität Wien, Austria, 2018).
42. J. P. Perdew, K. Burke and M. Ernzerhof, *Phys. Rev. Lett.* **77**, 3865 (1996).
43. F. Tran and P. Blaha, *Phys. Rev. Lett.* **102**, 226401 (2009).
44. H. J. Monkhorst and J. D. Pack, *Phys. Rev. B* **13**, 5188 (1976).
45. P. E. Blöchl, O. Jepsen and O. K. Andersen, *Phys. Rev. B* **49**, 16223 (1994).
46. R. P. Feynman, *Phys. Rev.* **56**, 340 (1939).
47. F. D. Murnaghan, *Proc. Natl. Acad. Sci.* **30**, 244 (1944).
48. B. Kuchta, L. Firlej and R. Etters, An influence of the pressure on metastability of the HCP phase of solid nitrogen, in *Frontiers of High Pressure Research II: Application of High Pressure to Low-Dimensional Novel Electronic Materials*, NATO Science Series (Series II: Mathematics, Physics and Chemistry), Vol. 48 (Springer, Dordrecht, 2001), pp. 251–261.
49. R. Hill, *Proc. Phys. Soc. A* **65**, 349 (1952).
50. M. Born and K. Huang, *Dynamical Theory of Crystal Lattices* (Clarendon Press, 1954).
51. S. Pugh, *Lond. Edinb. Dublin Philos. Mag. J. Sci.* **45**, 823 (1954).
52. I. Frantsevich, F. Voronov and S. Bokuta, in *Elastic Constants and Elastic Moduli of Metals and Insulators Handbook* (Naukova Dumka, Kiev, 1983), pp. 60–180.
53. J. Kübler, *Physica B+ C* **127**, 257 (1984).
54. L. Pauling, *The Nature of the Chemical Bond and the Structure of Molecules and Crystals: An Introduction to Modern Structural Chemistry* (Cornell University Press, 1960).